Protected biofactors and antioxidants reduce the negative consequences of virus and cold challenge while enhancing performance by modulating immunometabolism through cytoskeletal and immune signaling in the jejunum

F. Perry [*], L. Lahaye,[†] E. Santin,[†] C. Johnson,[*] D. R. Korver,[‡] M. H. Kogut [§], and R. J. Arsenault[*,1]

[*]*Department of Animal and Food Sciences, University of Delaware, DE, USA;* [†]*Jefo Nutrition Inc., Saint-Hyacinthe, QC, Canada;* [‡]*University of Alberta, Edmonton, AB, Canada; and* [§]*USDA-ARS, Southern Plains Agricultural Research Center, College Station, TX, USA*

ABSTRACT The aim of this study was to evaluate the effectiveness and mechanism of action of 2 feed additives in reducing the impacts of virus and temperature stressors. We determined the effects of protected biofactors and antioxidants (**P(BF+AOx)**), and protected biofactors and antioxidants with protected organic acids and essential oils (**P(BF+AOx)+P(OA+EO)**) on the immune and metabolic health of Ross 308 broiler chickens. These biofactors and antioxidants were derived from vitamins, and *Aspergillus niger, Aspergillus oryzae* and *Bacillus subtilis* fermentation extracts. All Ross 308 chickens were exposed to a double-dose of live bronchitis vaccine at d 0 and environmentally challenged by reducing the temperature from 32°C to 20°C at d 3 for 48 h. Control birds were fed without feed additives in the diet. Performance data and jejunum samples were collected to evaluate the effects of these treatments on growth, cytokine expression, and protein phosphorylation via kinome peptide array. ANOVA was used for statistical analysis of the performance and gene expression data (p-value of 0.05), and PIIKA2 was used for statistical evaluation and comparison of the kinome peptide array data. The P(BF plus;AOx) and P(BF+AOx)+P(OA+EO) treatments significantly increased bird weight gain and decreased feed conversion. The kinome peptide array data analysis showed increased activity of cytoskeletal, cell growth and proliferation proteins, and metabolic signaling in the jejunum of P(BF+AOx)+P(OA+EO) treated chickens. There was a significant decrease in IL-6 gene expression in the jejunum of P(BF+AOx)+P(OA+EO) samples compared to control at d 15. P(BF+AOx)+P(OA+EO) treatments in the jejunum showed strong immunomodulatory effects, perhaps to control inflammation. P(BF+AOx)+P(OA+EO) improves gut health via growth and metabolic signaling in the jejunum while inducing stronger immunomodulation.

Key words: immunometabolism, kinome peptide array, protected biofactors and antioxidants, cold stress, gut health

2022 Poultry Science 101:102172
https://doi.org/10.1016/j.psj.2022.102172

INTRODUCTION

Poultry is the most widely consumed meat in the world (OECD and Food and Agriculture Organization of the United Nations, 2021) and broiler chickens are the predominant source of this product (OECD/FAO, 2022; OECD and Food and Agriculture Organization of the United Nations, 2021). Per 2018 estimates, poultry production and exports are set to increase both in the United States and worldwide (OECD/FAO, 2022) to match the increasing demand for poultry meat. It is projected that global poultry consumption will increase to 152 million tonnes or more from 2021 to 2030 (OECD and Food and Agriculture Organization of the United Nations, 2021). The quality and formulation of feed is important to meeting market demands and producers' goals of increasing average daily gains (**ADG**) and reduced feed conversion ratio (**FCR**) of broilers; especially following government restrictions on antibiotics in many countries, and addressing consumers concerns about animal welfare. However, there are factors that may not be within the control of the producer that can induce biological stress responses and negatively impact health and growth. Poultry researchers have developed many intervention strategies to boost birds' immune response to infections and stressors (Swaggerty et al., 2019). Temperature stress can have severe performance and health related effects on commercial broilers (Zhang et al., 2016). While in much of the world heat stress is

Received June 1, 2022.
Accepted August 30, 2022.

[1]Corresponding author: rja@udel.edu

the predominant concern, in northern broiler producing nations, cold stress is often a more severe production limiting issue (Hangalapura et al., 2003). Meanwhile respiratory infections, the most predominant of which in many locations is infectious bronchitis virus (**IBV**), can degrade performance directly or due to secondary infections (Jackwood and De Wit, 2013) resulting in energy being redirected to mucosal immune response and away from growth. Feed ingredients play an important role in the regulation of birds' biological responses to unfavorable events as it is the source of energy and metabolites birds require for all cellular and system processes and determines the robustness of immune responses and growth. These immune responses require the activation of key metabolic pathways, thus the concept of immunometabolism is a critical consideration in poultry nutrition (Arsenault and Kogut, 2015). Feed additives and formulations can act to improve poultry responses to environmental and immune challenges, and we can improve these responses by understanding their mechanisms of action. Herein, we compared the effects of feed additives on the immune and metabolic health of birds that have been challenged with IBV and environmental cold stress, using performance metrics, the kinome peptide array technique and gene expression. The kinome peptide array uses species-specific and process-specific kinase target peptides printed on a glass array; these target peptides can be phosphorylated by active kinases in the biological samples (Arsenault et al., 2011; Daigle et al., 2014; Arsenault and Kogut, 2015). The phosphorylation of these peptides can be measured and visualized to determine changes in signaling cascades in a sample which may alter biological functions and activities (Arsenault and Kogut, 2015). The objective of this study was to evaluate and compare the immunometabolic effects and mechanisms of action of 2 feed additives, protected biofactors and antioxidants (**P(BF+AOx)**), and protected biofactors and antioxidants with protected organic acids and essential oils (**P(BF+AOx)+P(OA+EO)**) in broilers exposed to an early life cold stress and immune stimulation; and to identify their mechanism of action in the broiler gut. Previous research showed (P(BF+AOx) induced changes in the immunometabolic profile of both liver and jejunum samples (Bortoluzzi et al., 2021). This paper focuses on the differences and similarity between (P(BF+AOx) and (P(BF+AOx)+P(OA+EO) treatments in the jejunum, with more emphasis on the kinomic profile.

MATERIALS AND METHODS

Birds, Housing, and Treatments

At the hatchery, 1,080 one-day old male Ross × Ross 308 chickens were vaccinated against Marek's disease (HVT). The trial was conducted at the experimental station of Jefo Nutrition Inc., in Saint-Hyacinthe, QC, Canada. The feeding program was divided into 2 phases: starter (0−14 d) and grower (14−35 d). The feed formulation was corn and soybean meal based (Table 1); feed additives were mixed separately in the feed. The experiment consisted of 3 treatment groups: treatment 1; control, treatment 2; P(BF+AOx), and treatment 3; P(BF+AOx)+P(OA+EO). Treatments 2 and 3 were feed additives that contained mixtures of protected Biofactors and Antioxidants (P(BF+AOx)) (Jefo Nutrition Inc.) given to chickens from d 1 to 14. The experimental diets follow the NRC guidelines (NRC, 1994) for all experimental diets.

Briefly, the protected biofactors and antioxidants P(BF+AOx) were derived from a complex of vitamins and fermentation extract of vitamin A, vitamin D_3, vitamin E, menadione, thiamine, riboflavin, niacin, pantothenic acid, vitamin B_6, biotin, folic acid, vitamin B_{12}, L-tryptophan, and fermentation extract of dried *Bacillus subtilis, Aspergillus niger*, and *Aspergillus oryzae*. The P(BF+AOx)+P(OA+EO) formulation comprised the P(BF+AOx) formulation plus organic acids (citric acid, malic acid, sorbic acid, fumaric acid) and essential oils (thymol, eugenol, and vanillin). The P(BF+AOx)+P(OA+EO) active compounds were microencapsulated in a matrix of triglycerides from hydrogenated vegetable oil (Jefo Nutrition Inc.) (Table 1).

Each treatment consisted of 12 replicate pens with 30 birds each. The birds were placed onto floor pens with new litter. Each pen was provided with supplemental heat, and ad libitum access to water and feed in mash form.

Challenge

On d 0, all the birds received a double-dose of live bronchitis vaccine (**MILDVAC-Ma5**) at the hatchery. On d 3 all the chickens were submitted to an acute cold stress for 48 h with temperature between 20 and 23°C (or 9 to 12°C below the thermoneutral temperature for this age) and returned to a normal temperature afterward (Bortoluzzi et al., 2021).

Sample Collection

At 7 and 15 d, jejunum samples were collected from 6 birds per experimental group to evaluate the expression of immune-related genes. Jejunum samples from 3 of the d 15 birds per experimental group were harvested and immediately flash frozen in liquid nitrogen to preserve kinase enzymatic activity and stored at −80°C prior to further processing. Samples were shipped overnight on dry ice to the Kinome Center at University of Delaware, for kinome peptide array analysis.

Gene Expression

Jejunum samples were evaluated for expression of immune-related genes, according to Kogut and Arsenault (2015). Briefly, the mRNA was isolated from 25 mg of tissue using the RNeasy Plus mini kit (Qiagen, Hilden, Germany). The total isolated mRNA was eluted with 50 μL of RNase-free water and stored at −80°C for

Table 1. Starter (1−21 d) and grower (21−35 d) diets formulation, and formulated energy and nutrient composition.

Ingredient, %	Starter control	Starter treatment	Grower control	Grower treatment
Corn	30.6	30.6	34.0	34.0
Soybean meal, 48% CP	26.0	26.0	18.3	18.3
Wheat	31.0	31.0	34.3	34.3
DDGS	5.0	5.0	5.0	5.0
Animal fat	2.8	2.8	4.4	4.4
Monocalcium phosphate	0.98	0.98	1.01	1.01
Calcium carbonate	2.13	2.13	1.73	1.73
NaCl	0.31	0.31	0.28	0.28
L-lysine HCl	0.315	0.315	0.310	0.310
DL-Methionine, 99%	0.305	0.305	0.245	0.245
L-threonine	0.090	0.090	0.045	0.045
Choline, 60%	0.076	0.076	0.076	0.076
L-Valine	0.259	0.259	0.076	0.076
L-Tryptophane	0.029	0.029	0.024	0.024
Vitamin-Mineral Premix[1]	0.15	0.15	0.15	0.15
Sodium bicarbonate	-	-	0.04	0.04
P(BF+AOx)[2] or	-	0.015 or	-	0.015 or
P(BF+AOx)+P(OA+EO)[3]		0.015 + 0.01		0.015+0.01
Formulated energy and nutrient composition				
ME Kcal/Kg	2,950	2,950	3,097	3,097
Crude Protein, %	20.5	20.5	17.5	17.5
Fat, %	5.34	5.34	6.98	6.98
Lysine, %	1.200	1.200	1.003	1.003
Thr, %	0.797	0.797	0.639	0.639
Met+Cys, %	0.938	0.938	0.810	0.810
Non phytate phosphorus, %	0.440	0.440	0.440	0.440
Total Ca, %	1.11	1.11	0.95	0.95
Na, %	0.15	0.15	0.15	0.15

[1]Supplied per kg of diet: vitamin A, 10,005 IU; vitamin D_3, 3,000 IU; vitamin E, 30 IU; vitamin K, 2.55 mg; vitamin B_{12}, 15 mg; biotin, 201 mg; thiamine, 3 mg; riboflavin, 6 mg; pantothenic acid, 14.1 mg; pyridoxine, 3.6 mg; niacin, 49.95 mg; folic acid, 1 mg; Zn, 100; Fe, 49.5 mg; Cu, 15 mg; I, 0.09 mg; Se, 0.45 mg, Mn, 100 mg.

[2]Supplied per kg of diet: vitamin A, 900 IU; vitamin D_3, 450 IU; vitamin E, 12 IU; vitamin K, 0.135 mg; vitamin B_{12}, 0.00525 mg; biotin, 0.03 mg; thiamine, 0.9 mg; riboflavin, 1.35 mg; pantothenic acid, 3 mg; pyridoxine, 0.75 mg; niacin, 12 mg; folic acid, 0.3 mg.

[3]The P(BF+AOx)+P(OA+EO) formulation comprised the P(BF+AOx) formulation plus 0.01% organic acids (citric acid, malic acid, sorbic acid, fumaric acid) and essential oils (thymol, eugenol, and vanillin) microencapsulated in a matrix of triglycerides from hydrogenated vegetable oil.

qRT-PCR analysis. RNA was quantified and the quality evaluated using a spectrophotometer (NanoDrop Products, Wilmington, DE).

The PCR was performed using the TaqMan fast universal PCR master mix and one-step RT-PCR master mix reagents (Applied Biosystems, Waltham, MA). Normalization was carried out using 28S rRNA as a housekeeping gene, and the corrected cytokine mean change in mRNA levels were calculated as follow: mean 40-Ct*slope of the standard curve of the target cytokine/ slope of the standard curve of the 28S gene*differential factor of the 28S gene (Arsenault and Kogut, 2015). Jejunum samples were tested for IL-6 and IL-10. The prime and probe sets used in the qRT-PCR are reported in Bortoluzzi et al. (2021).

Kinome Peptide Array

The kinome peptide array was performed as described by (Johnson et al., 2019). Forty (40) mg of samples were lysed using bead-based homogenization in 100 μL of lysis buffer containing protease and phosphatase inhibitors. The lysed tissue samples were incubated on ice and then spun down in a refrigerated microcentrifuge at 14,000 *g* for 10 min at 4°C. An aliquot of supernatant was mixed with 10 μL of activation mix containing ATP as the phosphate group donor. Eighty μL of the supernatant-activation mix solution was applied to the peptide microarray. The custom-designed peptide arrays were obtained from JPT Peptide Technologies (Berlin, Germany), based on our sequence designs. A 25 × 60 mm, glass lifter slip was then applied to the microarray to sandwich and disperse the applied lysate.

Microarrays were then incubated in a humidity chamber at 40°C and 5% CO^2. Arrays were then placed in a 50 mL centrifuge tube containing phosphate-buffered saline (**PBS**)−1% Triton, to remove the lifter slip from the microarray surface. Arrays were then submerged in 2M NaCl-1% Triton and agitated for a minimum of 30 s. This process was then repeated with fresh 2M NaCl-1% Triton. Arrays were given a final wash in double distilled water with agitation.

Array slides were submerged in phosphospecific fluorescent ProQ Diamond Phosphoprotein Stain (Life Technologies, Carlsbad, CA) in a large dish and placed on a shaker table at 50 rpm for 1 h. Arrays were then placed in a new dish and submerged in destain solution (20% acetonitrile (EMD Millipore Chemicals, Billerica, MA) and 50 mM sodium acetate [Sigma Aldrich, St. Louis, MO]) for 10 min with agitation at 50 rpm. This process was repeated 2 times. A final wash was performed with double distilled water. The arrays were spun dried. Arrays were then scanned using a Tecan PowerScanner microarray scanner (Tecan Systems, San Jose, CA) at 532 to 560 nm with a 580 nm filter to detect dye fluorescence to collect the array image.

Kinome Peptide Array Data Analysis

Images were gridded using GenePix Pro software, and the spot intensity signal collected as the mean of pixel intensity using local feature background intensity calculation with the default scanner saturation level. The resultant data was then analyzed by the PIIKA2 peptide array analysis software (http://saphire.usask.ca/saphire/piika/index.html) (Trost et al., 2013). Briefly, the resulting data points were normalized to eliminate variance due to technical variation, for example, random variation in staining intensity between arrays or between array blocks within an array. Variance stabilization normalization was performed. Using the normalized data set comparisons between treatment and control groups was performed, calculating fold change and a significance *P*-value. The *P*-value was calculated by conducting a one-sided paired *t* test between treatment and control values for a given peptide. The resultant fold change and significance values were then used to generate higher order analysis (heatmaps, hierarchical clustering, principal component analysis, pathway analysis, etc.).

The kinome peptide array analysis was performed in triplicate for each group per tissue. A total of 9 samples, 3 per group were used for kinome peptide array analysis. Three treatment (cold stress and IBV vaccine challenged broilers given feed additives) vs. control (cold stress and IBV vaccine challenged broilers without feed additives) combinations (Table 2) were used to generate kinome profiles of these samples.

As described by Perry et al. (2020), post PIIKA2 analysis was performed using the following online databases and tools; STRING database (Szklarczyk et al., 2019) Kyoto Encyclopedia of Genes and Genomes (**KEGG**) pathways and KEGG color and search pathways (Kanehisa and Sato, 2020), PhosphoSitePlus (Hornbeck et al., 2015), Uniprot (The UniProt Consortium, 2021), and Venny 2.1 (Oliveros, 2007).

Table 2. Treatment vs. control combination for the kinome profile analysis.

Treatment[1] [2]	Control[2]
Jejunum P(BF+AOx)+P(OA +EO) d 15,	Jejunum Control (challenge only) d 15
Jejunum P(BF+AOx) d 15	Jejunum Control (challenge only) d 15
Jejunum P(BF+AOx)+P(OA +EO) d 15	Jejunum P(BF+AOx) d 15

[1]Protected biofactors and antioxidants P(BF+AOx), protected biofactors and antioxidants with protected organic acids and essential oils P(BF+AOx)+P(OA+EO).
[2]From each experimental group samples of N = 3 kinome were collected for analysis.

Statistical Analysis

A two-way ANOVA was used for statistical analysis of the performance data via the SAS software (SAS 9.4). The data were tested for normality and homogeneity. Nonparametric data were submitted to the Kruskal-Wallis test ($P < 0.05$). A one-way ANOVA and Tukeys post-hoc test was used for statistical analysis of the gene expression data via the JMP software (JMP Pro 16). All *P*-values lower than or equal to 0.05 were considered statistically significant. *P*-values greater than 0.05 but less than or equal to 0.1 indicate a trend to statistical significance. The European Production Efficiency Factor (**EPEF**) was calculated as described by Bortoluzzi et al., 2021, using the formula: body weight (Kg) × % survivability × 100/FCR × trial duration in days.

RESULTS

Effects of Treatments on Performance

Both P(BF+AOx) and P(BF+AOx)+P(OA+EO) fed birds showed significant increase in BWG compared to control (Table 3), with the exceptions from 0 to 21 d

Table 3. Growth performance of control and antioxidant+ biofactors treated birds.

Meaasurement[1]	Control	P(BF+AOx)	P(BF+AOx)+P(OA+EO)	SEM	*P*-value
BWG 0−7 d[3]	92[b]	95[a]	98[a]	1.33	**0.002**
FI 0−7 d[3]	118	117	120	0.86	0.39
FCR 0−7 d	1.266[a]	1.229[b]	1.226[b]	0.01	**0.02**
BWG 0−14 d[3]	345[b]	359[a]	359[a]	3.68	**0.007**
FI 0−14 d[3]	456	469	470	3.51	0.54
FCR 0−14 d	1.322	1.306	1.31	0.01	0.19
BWG 0−21 d[3]	770[b]	799[a]	783[ab]	6.96	**0.007**
FI 0−21 d[3]	1069	1096	1088	7.2	0.55
FCR 0−21 d	1.389[a]	1.372[b]	1.385[ab]	0.01	**0.02**
BWG 0−28 d[3]	1367[b]	1422[a]	1393[ab]	11.43	**0.002**
FI 0−28 d[3]	2042	2107	2085	14.44	0.73
FCR 0−28 d	1.545[a]	1.516[b]	1.533[a]	0.01	**0.001**
BWG 0−35 d[3]	2,051[b]	2,136[a]	2,108[a]	20.15	**0.008**
FI 0−35 d[3]	3,281	3,390	3,363	24.93	0.16
FCR 0−35 d	1.686[a]	1.647[b]	1.663[ab]	0.01	**0.03**
EPEF[2]	358.4	373.03	370.13	5.76	0.22
Survival rate	0.98	0.97	0.97	0.01	0.35

Boldface pathways are discussed in further detail in this paper.
[1]Abbreviations: BWG, body weight gain; FI, feed intake; FCR, feed conversion ratio.
[2]European Production Efficiency Factor, body weight (Kg) × % survivability × 100/FCR × trial duration in days.
[3]Measured in grams (g).
[a,b]$P < 0.05$.

Table 4. The top 20 list of KEGG pathways in P(BF+AOx)+P(OA+EO) treated jejunum relative to control.

P(BF+AOx)+P(OA+EO)[1] Day 15Top 20 KEGG pathways[2]	Observed protein count	False discovery rate
MAPK signaling pathway	**56**	**1.02E-39**
Pathways in cancer	65	6.09E-37
PI3K-Akt signaling pathway	55	1.46E-35
Insulin signaling pathway	37	4.48E-31
Ras signaling pathway	**41**	**3.20E-28**
Central carbon metabolism in cancer	27	1.61E-26
Proteoglycans in cancer	36	3.83E-25
Focal adhesion	**36**	**4.58E-25**
Hepatitis B	32	1.02E-24
Neurotrophin signaling pathway	30	1.08E-24
Insulin resistance	29	2.17E-24
MicroRNAs in cancer	32	2.80E-24
ErbB signaling pathway	26	2.91E-23
Kaposi's sarcoma-associated herpesvirus infection	33	5.32E-23
Rap1 signaling pathway	**34**	**8.14E-23**
EGFR tyrosine kinase inhibitor resistance	25	1.18E-22
Osteoclast differentiation	28	7.25E-22
Acute myeloid leukemia	23	1.42E-21
Chemokine signaling pathway	**31**	**3.93E-21**
AMPK signaling pathway	**27**	**4.08E-21**

Boldface pathways are discussed in further detail in this paper.
[1]Protected biofactors and antioxidants with protected organic acids and essential oils P(BF+AOx)+P(OA+EO)
[2]The significantly phosphorylated peptides generated from the *t* test performed by PIIKA2 were entered into the STRING database. The list of Kyoto Encyclopedia of Genes and Genomes (KEGG) pathways were downloaded and analyzed for common and/or relevant immune or metabolic pathways.

Table 5. The top 20 list of KEGG pathways in P(BF+AOx) treated jejunum relative to control.

P(BF+AOx)[1] Day 15Top 20 KEGG pathways[2]	Observed protein count	False discovery rate
MAPK signaling pathway	**35**	**9.19E-25**
Pathways in cancer	43	9.19E-25
Focal adhesion	**29**	**9.59E-23**
Hepatitis B	26	1.50E-22
ErbB signaling pathway	22	4.30E-22
FoxO signaling pathway	**24**	**5.38E-21**
Neurotrophin signaling pathway	23	7.86E-21
Proteoglycans in cancer	27	7.86E-21
PI3K-Akt signaling pathway	32	5.60E-20
Central carbon metabolism in cancer	19	5.61E-20
Insulin signaling pathway	23	1.01E-19
Kaposi's sarcoma-associated herpesvirus infection	25	2.43E-19
EGFR tyrosine kinase inhibitor resistance	19	8.22E-19
Ras signaling pathway	**26**	**2.07E-18**
MicroRNAs in cancer	22	1.00E-17
Rap1 signaling pathway	**24**	**2.35E-17**
Glioma	17	4.26E-17
Osteoclast differentiation	20	7.53E-17
Relaxin signaling pathway	**20**	**1.63E-16**
Cellular senescence	**21**	**2.68E-16**

Boldface pathways are discussed in further detail in this paper.
[1]Protected biofactors and antioxidants P(BF+AOx)+P(OA+EO).
[2]The significantly phosphorylated peptides generated from the *t* test performed by PIIKA2 were entered into the STRING database. The list of Kyoto Encyclopedia of Genes and Genomes (KEGG) pathways were downloaded and analyzed for common and/or relevant immune or metabolic pathways.

and 0 to 28 d, where P(BF+AOx)+P(OA+EO)-fed birds were not significantly different from control or P(BF+AOx) treated birds (Table 3). P(BF+AOx) showed statistically significant reduction in FCR compared to control from 0 to 7, 0 to 21, 0 to 28, and 0 to 35 d, while P(BF+AOx)+P(OA+EO) showed a statistically significant reduction only from 0 to 7 d with no change in FCR when compared to control or P(BF+AOx) from 0 to 14 and 0 to 35 d. There was no effect of treatment on feed intake (**FI**) across all groups. The same can be said for survival rate and European production efficiency factor (**EPEF**).

Treatment Effects on Signaling Profile

Functional analysis of the phosphorylation data showed that both treatments altered the immunometabolic profiles of the jejunum via MAPK signaling which encompasses growth, inflammatory and cell cytoskeleton signaling (Tables 4 and 5). To understand the effects and changes these treatments induced in the signaling cascades within the broiler jejunum compared to challenge alone, the list of all significantly phosphorylated proteins for each treatment vs. control pair was entered into STRING database. The lists of KEGG pathways were then extracted from the STRING database and sorted by false discovery rate (**FDR**) in ascending order. The lists of top 20 KEGG pathways for each treatment compared to control are reported in Tables 4 and 5. Each treatment significantly altered several different biological pathways of the respective tissues. Many of the pathways shown in the lists are immunometabolic pathways that are downstream of growth receptors and are important in the regulation of inflammation, cell communication, cell cytoskeleton, and metabolism during stress response. More specifically, both jejunum samples showed pathways involved in cytoskeleton regulation and cell growth such as Rap1 signaling, Ras signaling, and focal adhesion signaling (Table 4).

There were differences in P(BF+AOx)+P(OA+EO) and P(BF+AOx) signaling. The signaling pathways **Cellular Senescence** and **Relaxin Signaling** were observed in the top 20 KEGG pathways of the jejunum

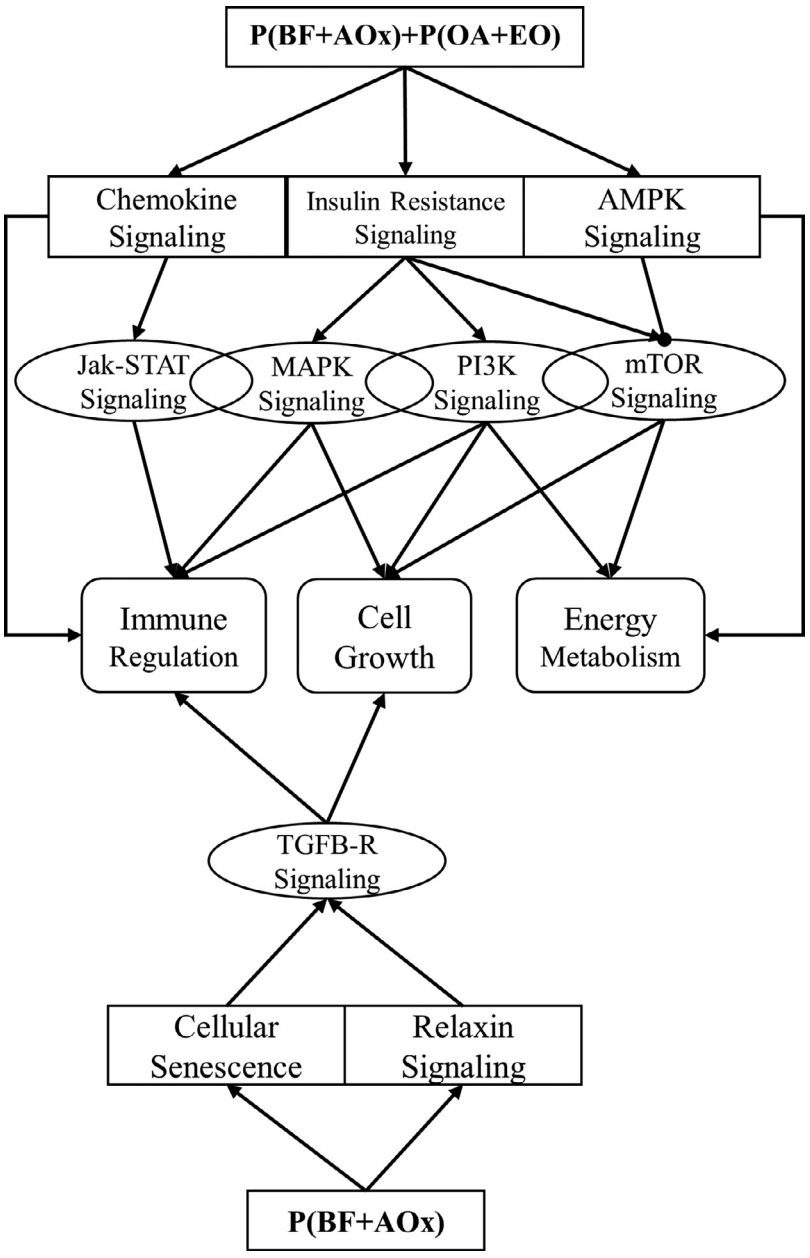

Figure 1. Schematic of immunometabolic pathways processes induced by feed additives in the jejunum. This schema illustrates the different immunometabolic pathways altered by each feed additive and the signal transduction cascades these pathways have in common that lead to changes in key immunometabolic processes. The pathways in this schema were derived by comparing the list of top 20 KEGG pathways for each feed additive in the jejunum for differences.

P(BF+AOx) but not in P(BF+AOx)+P(OA+EO) (Figure 1, Tables 4 and 5). These two pathways are linked via TGF-beta receptor signaling pathway which is characterized by the secretion of inflammatory cytokines and growth receptors signaling. In the top 20 KEGG pathways of P(BF+AOx)+P(OA+EO), we observed **Insulin resistance, chemokine** and **AMPK signaling Pathways** that were not observed in the top 20 of jejunum P(BF+AOx) (Figure 1). Chemokine signaling involves the stimulation of cytokine production and cell growth factors via MAPK and Jak-STAT signaling. Insulin resistance and AMPK signaling both involve the regulation of energy metabolism via mTOR and PI3K signaling. Besides the differences in the number of proteins involved in MAPK signaling between the 2 treatments, we also observed more protein counts in P(BF+AOx)+P(OA+EO) KEGG pathways than P(BF+AOx) KEGG pathways (Tables 4 and 5). These differences between treatments show stronger immunometabolic effects of P(BF+AOx)+P(OA+EO) in the jejunum.

Effects of P(BF+AOx)+P(OA+EO) Compared to P(BF+AOx)

To determine the impact of P(BF+AOx)+P(OA+EO) in chickens compared to P(BF+AOx), PIIKA2 comparisons were ran using P(BF+AOx)+P(OA+EO) as the treatment and P(BF+AOx) as the control as shown in Table 2. After further analysis as previously described, the top 20 KEGG pathways for jejunum

Table 6. The top 20 list of KEGG pathways in the jejunum P (BF+AOx)+P(OA+EO)[1] treatment groups relative to P(BF +AOx)[2].

KEGG pathways[3]	Observed protein count	False discovery rate
MAPK signaling pathway	**60**	**6.58E-42**
Pathways in cancer	72	3.47E-41
PI3K-Akt signaling pathway	56	1.92E-34
Insulin signaling pathway	37	1.26E-29
Central carbon metabolism in cancer	29	5.02E-28
Hepatitis B	36	7.32E-28
MicroRNAs in cancer	35	3.65E-26
Ras signaling pathway	39	8.61E-25
Neurotrophin signaling pathway	31	1.18E-24
Proteoglycans in cancer	36	6.29E-24
Kaposi's sarcoma-associated herpesvirus infection	35	9.69E-24
ErbB signaling pathway	27	1.91E-23
Focal adhesion	34	7.58E-22
Toll-like receptor signaling pathway	**27**	**1.61E-21**
AMPK signaling pathway	**28**	**4.39E-21**
Insulin resistance	**27**	**4.39E-21**
Rap1 signaling pathway	33	1.37E-20
EGFR tyrosine kinase inhibitor resistance	24	1.61E-20
Human papillomavirus infection	39	1.69E-20
Prostate cancer	25	7.87E-20

Boldface pathways are discussed in further detail in this paper.

[1]Protected biofactors and antioxidants with protected organic acids and essential oils P(BF+AOx)+P(OA+EO).

[2]Protected biofactors and antioxidants P(BF+AOx).

[3]The significantly phosphorylated peptides generated from the *t* test performed by PIIKA2 were entered into the STRING database. The list of Kyoto Encyclopedia of Genes and Genomes (KEGG) pathways were downloaded and analyzed for common and/or relevant immune or metabolic pathways.

samples are reported in Table 6. Table 6 shows the signaling pathways due to significant changes in phosphorylation by P(BF+AOx)+P(OA+EO) treatment in the jejunum compared to P(BF+AOx). Most of these pathways are part of the MAPK cell growth and energy metabolism signal transduction cascades previously mentioned except for the **Toll-like receptor signaling pathway**, an innate immune pathway that plays a critical role in recognizing pathogens (Table 6). It is important to remember that the activation status of each protein in these pathways cannot be assumed by the information provided in Tables 4–6, and Figure 1. Detailed analysis of the phosphorylation sites of each protein is necessary to fully understand the effects of these treatments on the activation status of these proteins and to determine the immunometabolic mechanism of action in the jejunum.

Effects on Cytoskeleton Regulation

The lists of top 20 KEGG pathways for each group showed that the treatments induced significant changes in cell motility, cell migration and cytoskeletal regulation compared to control (challenge alone) (Tables 4 and 5). Therefore, regulation of actin cytoskeleton, a pathway that includes the major cytoskeleton and cellular junction proteins was further analyzed. Analysis of the regulation of the actin cytoskeleton pathway for each treatment showed that P(BF+AOx)+P(OA+EO) treatment positively affects actin and myosin contractility. Although the P(BF+AOx) treatment groups showed significant changes in cytoskeleton regulation proteins compared to control, the phosphorylation status of proteins like RHOA, ROCK, PAK, MLCK and others did not indicate significant changes in actin contractility and polymerization (Table 7). The direct comparison of P(BF+AOx)+P(OA+EO) to P(BF+AOx) revealed that, P(BF+AOx)+P(OA+EO) treatment induce increased activity of cytoskeletal regulatory proteins in the jejunum of broilers (Supplementary 1). Increased activation of microtubule regulators like SOS-1, Rac1, MEK2, IRSp53, and PPP2c-alpha was observed only for P(BF+AOx)+P(OA+EO) jejunum, supporting that P(BF+AOx)+P(OA+EO) induces more cytoskeletal changes in the jejunum.

Effects on Immunoregulation and Cell Death

The list of top 20 KEGG pathways for each treatment contained several pathways that involve signaling through cytokine receptors and the activity of many inflammatory proteins associated with immune response and regulation (Tables 4–6). Therefore, the effects of phosphorylation on the proteins involved in inflammatory and immune pathways like the **Chemokine, T**

Table 7. Effect of phosphorylation changes on major cytoskeleton regulation proteins.

Protein name	P(BF+AOx)+P(OA+EO)[1,2]	P(BF+AOx)[1,3]
Calmodulin	Inactive	Inactive
CAMK	Inactive	Active
EZ	Inactive	Inactive
FAK	Inactive	Inactive
MLCK	P	D
MYPT1	Inactive	Inactive
PAK	Inactive	D
Profilin 2	D	No change
PYK2	Active	No change
RHOA	Active	Active
ROCK	Active	No change
Stathmin	No change	Inactive

[1]The phosphorylation status of proteins in this table was determined by entering each protein's respective Uniprot accession into phosphosite, finding the annotation of the site of interest and accounting for the phosphorylation fold change (increased or decreased) of that site. Active denotes increased phosphorylation of an inducing site or decreased phosphorylation on an inhibitory site. Inactive denotes decreased phosphorylation of an inducing site or increased phosphorylation on an inhibitory site. P denotes that the function of the site is unknown and the data shows increased phosphorylation. D denotes that the function of the site is unknown and the data shows decreased phosphorylation. No change denotes there were no statistically significant difference observe between treatment and control for that protein.

[2]Protected biofactors and antioxidants with protected organic acids and essential oils P(BF+AOx)+P(OA+EO).

[3]Protected biofactors and antioxidants P(BF+AOx).

Table 8. Effect of phosphorylation changes on major immunoregulation and cell death proteins.

Protein name	P(BF+AOx)+P(OA+EO)[1,2]	P(BF+AOx)[1,3]
AP-1/C-Fos	P	No change
B-ARRESTIN	P	P
BLNK	Inactive	Inactive
BTK	Inactive	Active
Caspase 3	Active	No change
Caspase 6	No change	Inactive
C-JUN	No change	Active
JNKK	Active	Active
MEKK3	Active	Active
NFAT	Active	Active
P38	Active	Active
PERK	Active	P
SMAD2/3	No change	Inactive
STAT1	Active	Active
SYK	Inactive	Inactive
TAK1	No change	No change
TBK	Inactive	Inactive
ZAP-70	Active	Active

[1]The phosphorylation status of proteins in this table was determined by entering each protein's respective Uniprot accession into phosphosite, finding the annotation of the site of interest and accounting for the phosphorylation fold change (increased or decreased) of that site. Active denotes increased phosphorylation of an inducing site or decreased phosphorylation on an inhibitory site. Inactive denotes decreased phosphorylation of an inducing site or increased phosphorylation on an inhibitory site. P denotes that the function of the site is unknown and the data shows increased phosphorylation. D denotes that the function of the site is unknown and the data shows decreased phosphorylation. No change denotes there were no statistically significant difference observe between treatment and control for that protein.

[2]Protected biofactors and antioxidants with protected organic acids and essential oils P(BF+AOx)+P(OA+EO).

[3]Protected biofactors and antioxidants P(BF+AOx).

cell receptor, and **Toll-like receptor** signaling pathways were further analyzed for a better understanding of how these treatments affect immunoregulation. When compared to control, P(BF+AOx) treatment group showed some critical changes in the activation status of inflammatory and cell death proteins via MAPK signaling and increased phosphorylation of these proteins on their active sites (Table 8). P(BF+AOx)+P(OA+EO) treatments induced a slightly different impact on cell death signaling indicated by the decreased inhibition of caspase 3 in the jejunum (Table 8). We also observed activation of caspases 3, 6, and 8 in the jejunum of P(BF+AOx)+P(OA+EO) groups when compared to P(BF+AOx).

The phosphorylation status of some cytokines and immune receptors were also analyzed and presented in Tables 9 and 10. The P(BF+AOx)+P(OA+EO) jejunum samples showed changes in the phosphorylation of more individual cytokines and immune receptors than P(BF+AOx) treatments. Many of these cytokines and immune receptors showed increased phosphorylation in the jejunum P(BF+AOx)+P(OA+EO) treated samples, while these same proteins in P(BF+AOx) treated jejunum samples showed decreased phosphorylation (Table 9).

The kinome peptide array data showed significant changes in the phosphorylation of IL-6 receptor

Table 9. Phosphorylation changes in major cytokines and immune receptors in jejunum P(BF+AOx)[1] at d 15.

Uniprot accession	Protein name	Human site	Chicken site	FC	*P*-value
P29460	Interleukin-12 subunit beta; IL-12B;	Y314	Y304	−1.06939	0.01631
P40189	**Interleukin-6 receptor subunit beta; IL-6R-beta;**	**S782**	**S757**	**1.08012**	**0.01624**
Q8N5C8	TAK1-binding protein 3; TAB-3;	T404	T403	1.07588	0.03082
Q12933	TNF receptor-associated factor 2; Tumor necrosis factor type 2 receptor-associated protein 3;	S11	S11	−1.05706	0.02792
P58753	Toll/interleukin-1 receptor domain-containing adapter protein; TIR domain-containing adapter protein;	Y86	Y77	−1.09435	0.00018
O15455	Toll-like receptor 3;	Y858	Y854	−1.11321	0.02742
O15455	Toll-like receptor 3;	Y759	Y754	−1.08145	0.037
Q9NR97	Toll-like receptor 8;	S939	S948	1.12636	0.00881
Q9UKE5	TRAF2 and NCK-interacting protein kinase;	S764	V730	−1.06118	0.03767
Q9NP60	X-linked interleukin-1 receptor accessory protein-like 2; IL-1-RAPL-2;	S343	S317	−1.08169	0.00305

Boldface pathways are discussed in further detail in this paper.

[1]Protected biofactors and antioxidants P(BF+AOx).

Table 10. Phosphorylation changes in major cytokines and immune receptors in jejunum P(BF+AOx)+P(OA+EO)[1] at d 15.

Uniprot accession	Protein name	Human site	Chicken site	FC	*P*-value
P29460	Interleukin-12 subunit beta; IL-12B;	Y314	Y304	−1.05492	0.01014
P40189	**Interleukin-6 receptor subunit beta; IL-6R-beta;**	**S782**	**S757**	**1.08541**	**0.01395**
P36897	TGF-beta receptor type-1; TGFR-1;	T200	T200	1.33268	0.00021
Q8N5C8	TAK1-binding protein 3; TAB-3;	T404	T403	1.10401	0.0024
Q8N5C8	TAK1-binding protein 3; TAB-3;	T404	T403	1.10401	0.0024
Q7L0 × 0	TLR4 interactor with leucine rich repeats;	T753	T721	1.20519	0
Q9Y4K3	TNF receptor-associated factor 6; Interleukin-1 signal transducer;	Y353	Y379	−1.11472	0.00186
P58753	Toll/interleukin-1 receptor domain-containing adapter protein; TIR domain-containing adapter protein;	Y86	Y77	−1.1929	0
Q15399	Toll-like receptor 1; Toll/interleukin-1 receptor-like protein; TIL;	Y691	Y704	1.08534	0.00059
Q6R5N8	Toll-like receptor 13;	S206	S78	−1.16332	0.00223
O15455	Toll-like receptor 3;	Y858	Y854	−1.25531	0
O60602	Toll-like receptor 5; Toll/interleukin-1 receptor-like protein 3;	Y798	Y800	1.04	0.04634
Q9NYK1	Toll-like receptor 7;	S610	T608	1.29188	0
Q9NR97	Toll-like receptor 8;	S939	S948	1.07154	0.0482
Q08881	Interleukin-2-inducible T-cell kinase; Tyrosine-protein kinase Lyk;	Y512	Y511	1.14335	0.00001

Boldface pathways are discussed in further detail in this paper.

[1]Protected biofactors and antioxidants with protected organic acids and essential oils P(BF+AOx)+P(OA+EO).

Table 11. Cytokine expression in the jejunum.

	Corrected cytokine means[1,2]				
Cytokines	Control	P(BF+AOx)	P(BF+AOx)+ P(OA+EO)	SEM	*P* value
IL-6	10.61[a]	8.18[ab]	**7.53[b]**	0.82	**0.05**
IL-10	7.07	6.12	7.75	0.63	0.12

Boldface pathways are discussed in further detail in this paper.
[1]Corrected cytokine means of IL-6 and IL-10 expression in jejunum samples at d 15.
[2]From each experimental group samples of N = 6 kinome were collected for analysis
[a,b]$P < 0.05$.

compared to control. Both P(BF+AOx) and P(BF +AOx)+P(OA+EO) showed increased phosphorylation of IL-6R. However, the cytokine gene data only showed a significant decrease in IL-6 gene expression (P 0.05) in the jejunum P(BF+AOx)+P(OA+EO) samples compared to control at day 15 (Table 11). No significant trends were observed for IL-10 expression, however, the pairwise comparison using Tukey's HSD showed a trend (P = 0.101) of decreased IL-10 expression in P(BF +AOx) compared to P(BF+AOx)+P(OA+EO).

Effect on Metabolic Signaling

Based on the result of our analysis, P(BF+AOx)+P (OA+EO) and P(BF+AOx) induced phosphorylation changes in cell growth and metabolic proteins in jejunum samples compared to control. Both P(BF+AOx) +P(OA+EO) and P(BF+AOx) treatments showed changes in energy metabolism proteins like AMPK, mTOR, HIF1-alpha, etc. Moreover, direct comparison of P(BF+AOX)+P(OA+EO) to P(BF+AOx) showed that P(BF+AOx)+P(OA+EO) induced significantly more activity in growth and metabolic signaling than P (BF+AOx). The top 20 KEGG pathways of P(BF +AOx)+P(OA+EO) compared to P(BF+AOx) clearly showed that P(BF+AOx)+P(OA+EO) had induced critical changes in cell cycle regulation and growth via insulin signaling and AMPK signaling pathways. Additionally, many changes in phosphorylation of cell growth proteins were observed in the jejunum P(BF+AOx)+P (OA+EO) compared to P(BF+AOx).

DISCUSSION

The performance data (Table 3) showed that treatment with both P(BF+AOx) and P(BF+AOx)+P(OA +EO) decreased FCR significantly. Performance data should be considered in the context that comparisons were made to a challenge (cold stress and IBV) control. Thus, an increase in performance suggests a decrease in the stress effects of the physiological and environmental challenge. Keeping in mind that the control in this study was a double-dose of viral vaccine and cold stress challenge, we wanted to understand the immunometabolic effects of changes in phosphorylation on key pathways. Therefore, signaling profiles of treatment groups were determined by detailed analysis of immunoregulatory, metabolic, cell growth, and cell cytoskeleton pathways that were observed in our KEGG analysis (Tables 4–7).

The kinome peptide array results showed significant changes in actomyosin contractility and focal adhesion. Specifically, jejunum samples collected from P(BF+ AOx)+P(OA+EO)−treated birds showed changes in the phosphorylation of ROCK, RHOA and MLCK which are orchestrators of actin and myosin contraction (Wu et al., 2010; Valencia-Expósito et al., 2016; Jin and Blikslager, 2020; Table 7 and Supplementary 1). The phosphorylation status of RHOA and ROCK indicate the inhibition of Myosin light chain phosphatase (**MLCP**), via phosphorylation by ROCK and the decrease phosphorylation of PAK attenuates its inhibition of Myosin light chain kinase (**MLCK;** Table 7), leading to actomyosin assembly and contraction. Another cytoskeleton signaling activity that was critically impacted by P(BF+AOx)+P(OA+EO) and P(BF +AOx) treatments was actin assembly, which involves polymerization and depolymerization of actin filaments; important for actin turnover which drives cell movement and shape. The decreased phosphorylation of profilin (Table 7), a driver of actin polymerization indicates its activation to facilitate the assembly of globular actin into filamentous actin (Sathish et al., 2004; Delorme et al., 2007; Zhang et al., 2011). Moreover, PAK which plays a key role in the activation of cofilin, the driver of actin depolymerization, was also less activated in P(BF +AOx)+P(OA+EO) jejunum (Callow et al., 2002). There were similar changes in focal adhesion signaling for both P(BF+AOx)+P(OA+EO) and P(BF+AOx) via Calmodulin, FAK and EZ. The overall difference in cytoskeletal regulation between P(BF+AOx)+P(OA +EO) and P(BF+AOx) was made clear via the changes in phosphorylation of MLCK, RHOA, ROCK and Profilin which were specific to P(BF+AOx)+P(OA+EO; Table 7 and Supplementary 1). Direct comparison of P(BF+AOx)+P(OA+EO) to P(BF+AOx) showed that P(BF+AOx)+P(OA+EO) induces more changes in cytoskeletal regulation in the jejunum (Supplementary 1). Thus, we concluded that P(BF+AOx)+ P(OA+EO) treatments induced more critical changes in the signaling of the cell cytoskeleton in the jejunum. These changes in cytoskeletal regulation are important for immune responses like phagocytosis and support cell movement during growth or development (Hall, 1994; Solaymani-Mohammadi and Singer, 2013; Würtemberger et al., 2020). Such changes may lead to increased gut barrier function in the P(BF+AOx)+P (OA+EO) treated birds by lessening acute inflammatory responses (Liu and Pope, 2004).

The kinome data indicated a strong effect of the 2 treatments on cellular response to stress (Table 8). Collectively, the proteins in Table 8 are involved in cellular response to stress via the stress activated protein kinase signaling pathway, MAPK (Bogoyevitch et al., 1996). Both treatments induced changes innate immune signaling and the pathways that link the adaptive and innate immune system. This is supported by changes in Toll-

like receptor signaling, chemokine signaling, Ras and Rap1 signaling, which involve signal transduction via T-cell receptor signaling. AP-1, JAK, STAT, NFAT, JNKK, MEKK3, P38, and ZAP-70 are some of the proteins involved in these pathways that were phosphorylated on their active sites for both treatments in the jejunum. P(BF+AOx)+P(OA+EO) induced more changes in the inflammatory profile in the jejunum because more changes were observed in the overall immune regulatory status. This includes changes in the cell death proteins, and linkers of adaptive and innate immunity proteins compared to control and P(BF+AOx; Table 8 and Supplementary 2). Increased activity of SOS, STAT, NF-kappa B, MEK, NFAT, p38, AP-1, ZAP-70, JNKK, IFN-R, TAB, TGFR, and more were observed in the jejunum samples of P(BF+AOx)+P(OA+EO) birds compared to control and P(BF+AOx; Table 8 and Supplementary 2). Increased activity of apoptotic proteins were observed in the jejunum samples of P(BF+AOx)+P(OA+EO) treated birds, specifically, caspases 3, 6, and compared to P(BF+AOx). Apoptosis is used to suppress pro-inflammatory responses such as necrosis and promote the release of anti-inflammatory factors by triggering phagocytosis of inflamed cells (Köröskényi et al., 2011; Szondy et al., 2017). The increased activity of apoptotic proteins in P(BF+AOx)+P(OA+EO) treated samples indicates its anti-inflammatory characteristics.

The phosphorylation status of IL-6R of P(BF+AOx)+P(OA+EO) and P(BF+AOx) treated jejunum samples showed increased phosphorylation (Tables 9 and 10), Gibson et al. (2000), showed that stimulation of the glycoprotein 130 (gp130) subunit of the IL-6 receptor (Table 9) results in the internalization of the receptor which triggers downstream activities. This gp130 is involved in inflammatory, immune, and metabolic regulation induced by IL-6 or IL-6 family of cytokines (Febbraio, 2007; White and Stephens, 2011; Cron et al., 2016). The gene expression results in P(BF+AOx) treated samples in the jejunum did not show any significant differences in IL-6 expression (Table 11). Because gp130 is stimulated by ligands other than IL-6, the phosphorylation of gp130 receptor as observed in the kinome peptide array results indicate metabolic downstream signaling via this receptor in P(BF+AOx) jejunum (Bortoluzzi et al., 2021). Thus, the immunometabolic effects of P(BF+AOx) is strongly dependent on signaling via the immunomodulatory cytokine receptor, IL-6R.

The gene expression results showed a decrease in IL-6 expression for P(BF+AOx)+P(OA+EO) jejunum samples (Table 11), however, the kinome peptide array results showed phosphorylation of the same IL-6 receptor gp130 subunit mentioned above (Table 10). These results suggest gp130 was stimulated by other ligands in the IL-6 family of cytokine like ciliary neurotrophic factor (**CNTF**) which acts on AMPK and insulin related signaling (White and Stephens, 2011). CNTF has also been shown to act on the AKT-mTOR-S6K signaling cascade (Ott et al., 2002). Therefore, despite the decreased expression of IL-6, the phosphorylation of gp130 in P(BF+AOx)+P(OA+EO) jejunum samples can be attributed to the metabolic effects of other ligands without inducing inflammation. Moreover, the increased activity of immune regulators in P(BF+AOx)+P(OA+EO) treated groups (Table 8 and Supplementary 2) indicate that this treatment improves immune responses independent of IL-6 and excessive pro-inflammatory signaling in the jejunum, perhaps via phagocytosis of apoptotic bodies of inflamed cells to reduce inflammation.

Table 12. Effects of phosphorylation changes on major growth and metabolic proteins.

PROTEIN	P(BF+AOx)+P(OA+EO)[1,2]	P(BF+AOx)[1,3]
AMPK	Active	Active
AKT	Active	Active
HIF	Active	Inactive
IRS	Inactive	Inactive
LKB1	No change	Inactive
MTOR	Active	No change
PDK	No change	Active
PKC	Active	Active
PKC-D	Active	No change
PP2A	Active	Active
PTEN	Inactive	Inactive
S6K1	Active	Active
4E-BP1	Inactive	No change
TSC2	D	No change

[1]The phosphorylation status of proteins in this table was determined by entering each protein's respective Uniprot accession into phosphosite, finding the annotation of the site of interest and accounting for the phosphorylation fold change (increased or decreased) of that site. Active denotes increased phosphorylation of an inducing site or decreased phosphorylation on an inhibitory site. Inactive denotes decreased phosphorylation of an inducing site or increased phosphorylation on an inhibitory site. P denotes that the function of the site is unknown and the data shows increased phosphorylation. D denotes that the function of the site is unknown and the data shows decreased phosphorylation. No change denotes there were no statistically significant difference observe between treatment and control for that protein.

[2]Protected biofactors and antioxidants with protected organic acids and essential oils P(BF+AOx)+P(OA+EO).

[3]Protected biofactors and antioxidants P(BF+AOx).

Moreover, there were changes in metabolic and growth signaling status of proteins in P(BF+AOx) treated birds and P(BF+AOx)+P(OA+EO) treated samples compared to control as observed in Table 12. We also observed critical changes in energy metabolism and cell growth when P(BF+AOx)+P(OA+EO) was compared to P(BF+AOx). Energy metabolism and cell growth are interdependent. As a cell undergoes cell growth and proliferation which involves mTOR, S6K, Sirt-1, Cdk2, Cdk6, and other anabolism proteins, it consumes a large sum of energy which can be generated via the signaling of AMPK, PGC-1 alpha, PPAR, PTEN, PFK, and other catabolism proteins (Supplementary 3). The proteins mentioned above showed changes in phosphorylation that led to increased activity in P(BF+AOx)+P(OA+EO) compared to P(BF+AOx) (Supplemental 3). This increase energy metabolism and consumption is true for immune regulation and response, and it is a key factor in immunometabolism. Thus, increase in energy metabolism is a result of and facilitates cell growth, immune signaling and cytoskeletal regulation as seen in Tables 7, 8, and 12 and

Supplementary 1, 2, and 3. Thus, these results suggest that P(BF+Ox)+P(OA+EO) had stronger effects on metabolism in the jejunum.

Before concluding, it is important to discuss the potential reasons AMPK and mTOR may both be active in the jejunum samples of P(BF+AOx)+P(OA+EO) treated birds. AMPK does not always directly phosphorylate mTOR to inhibit its activity (Garza-Lombó et al., 2018). Rather, AMPK phosphorylates tuberous sclerosis (TSC1/2) which phosphorylates and inhibits Rheb, preventing Rheb's activation of mTOR (Inoki et al., 2003). Akt can also phosphorylate and inhibit TSC, and kinome peptide array results show the phosphorylation of Akt on its active site for both treatment groups in the jejunum and the decreased phosphorylation of TSC in jejunum P(BF+AOx)+P(OA+EO) treated samples. Additionally, there are several proteins that phosphorylate and activate mTOR. And mTOR may indirectly regulate AMPK via S6K activity (Dagon et al., 2012). Thus, with the many intermediary and regulatory proteins between AMPK and mTOR, and the homeostatic cross-talk between the two proteins, the straightforward inhibitory effect of AMPK on mTOR is not always achievable. In some cases, both AMPK and mTOR activity is required to maintain a balanced catabolic and anabolic signaling during immunometabolic regulation as these results show, because a lack of balance may lead to negative effects (Garza-Lombó et al., 2018).

In conclusion, P(BF+AOx)+P(OA+EO) induced significantly more changes in the immunometabolic signaling of broiler chickens compared to P(BF+AOx). Specifically, P(BF+AOx)+P(OA+EO) altered the cytoskeletal activity and programmed cell death in the jejunum to promote gut health thus having a more homeostatic effect. Increased growth performance due to each treatment compared to control may be linked to changes in cell growth and metabolic signaling, P(BF+AOx)+P(OA+EO) appears to induce a unique effect in the growth and metabolic signaling in the gut compared to the P(BF+AOx) treatment. P(BF+AOx)+P(OA+EO) and P(BF+AOx) significantly altered the immunoregulatory signaling via adaptive and innate immunity to maintain a homeostatic immune response to cold stress and viral challenge without excessive inflammation, while P(BF+AOx)+P(OA+EO) displayed a less inflammatory response overall.

ACKNOWLEDGMENTS

This project was funded by Jefo Nutrition, St. Hyacinth, QC.

DISCLOSURES

L. Lahaye and E. Santin are employees and Jefo Nutrition. All other authors declare no conflict of interest.

SUPPLEMENTARY MATERIALS

Supplementary material associated with this article can be found in the online version at doi:10.1016/j.psj.2022.102172.

REFERENCES

Arsenault, R., P. Griebel, and S. Napper. 2011. Peptide arrays for kinome analysis: new opportunities and remaining challenges. Proteomics 11:4595–4609.

Arsenault, R. J., and M. H. Kogut. 2015. Immunometabolism and the kinome peptide array: a new perspective and tool for the study of gut health. Front. Vet. Sci. 2:1–5.

Bogoyevitch, M. A., J. Gillespie-Brown, A. J. Ketterman, S. J. Fuller, R. Ben-Levy, A. Ashworth, C. J. Marshall, and P. H. Sugden. 1996. Stimulation of the stress-activated mitogen-activated protein kinase subfamilies in perfused heart. Circ. Res. 79:162–173.

Bortoluzzi, C., L. Lahaye, F. Perry, R. J. Arsenault, E. Santin, D. R. Korver, and M. H. Kogut. 2021. A protected complex of biofactors and antioxidants improved growth performance and modulated the immunometabolic phenotype of broiler chickens undergoing early life stress. Poult. Sci. 100:101176.

Callow, M. G., F. Clairvoyant, S. Zhu, B. Schryver, D. B. Whyte, J. R. Bischoff, B. Jallal, and T. Smeal. 2002. Requirement for PAK4 in the anchorage-independent growth of human cancer cell lines. J. Biol. Chem. 277:550–558.

Cron, L., T. Allen, and M. A. Febbraio. 2016. The role of gp130 receptor cytokines in the regulation of metabolic homeostasis.J. Exp. Biol. 219:259–265.

Dagon, Y., E. Hur, B. Zheng, K. Wellenstein, L. C. Cantley, and B. B. Kahn. 2012. p70S6 kinase phosphorylates AMPK on serine 491 to mediate leptin's effect on food intake. Cell Metab 16:104–112.

Daigle, J., B. Van Wyk, B. Trost, E. Scruten, R. Arsenault, A. Kusalik, P. J. Griebel, and S. Napper. 2014. Peptide arrays for kinome analysis of livestock species. Front. Vet. Sci. 1:1–15.

Delorme, V., M. Machacek, C. DerMardirossian, K. L. Anderson, T. Wittmann, D. Hanein, C. Waterman-Storer, G. Danuser, and G. M. Bokoch. 2007. Cofilin activity downstream of Pak1 regulates cell protrusion efficiency by organizing lamellipodium and lamella actin networks. Dev. Cell 13:646–662.

Febbraio, M. A. 2007. gp130 receptor ligands as potential therapeutic targets for obesity. J. Clin. Invest. 117:841–849.

Garza-Lombó, C., A. Schroder, E. M. Reyes-Reyes, and R. Franco. 2018. mTOR/AMPK signaling in the brain: cell metabolism, proteostasis and survival. Curr. Opin. Toxicol. 8:102–110.

Gibson, R. M., W. P. Schiemann, L. B. Prichard, J. M. Reno, L. H. Ericsson, and N. M. Nathanson. 2000. Phosphorylation of human gp130 at Ser-782 adjacent to the Di-leucine internalization motif. Effects on expression and signaling. J. Biol. Chem. 275:22574–22582.

Hall, A. 1994. Small GTP-binding proteins and the regulation of the actin cytoskeleton. Annu. Rev. Cell Biol. 10:31–54.

Hangalapura, B. N., M. G. Nieuwland, G. de Vries Reilingh, M. J. Heetkamp, H. Van den Brand, B. Kemp, and H. K. Parmentier. 2003. Effects of cold stress on immune responses and body weight of chicken lines divergently selected for antibody responses to sheep red blood cells. Poult. Sci. 82:1692–1700.

Hornbeck, P. V., B. Zhang, B. Murray, J. M. Kornhauser, V. Latham, and E. Skrzypek. 2015. PhosphoSitePlus, 2014: mutations, PTMs and recalibrations. Nucleic Acids Res 43:D512–D520.

Inoki, K., T. Zhu, and K. L. Guan. 2003. TSC2 mediates cellular energy response to control cell growth and survival. Cell 115:577–590.

Jackwood, M. W., and S. De Wit. 2013. Pages 139−159 in Infectious Bronchitis in Diseases of Poultry. 13th ed. John Wiley & Sons, Inc, Hoboken, NJ ed. D. E. Swayne.

Jin, Y., and A. T. Blikslager. 2020. The regulation of intestinal mucosal barrier by myosin light chain kinase/Rho kinases. Int. J. Mol. Sci. 21:3550–3567.

Johnson, C. N., M. H. Kogut, K. Genovese, H. He, S. Kazemi, and R. J. Arsenault. 2019. Administration of a postbiotic causes

immunomodulatory responses in broiler gut and reduces disease pathogenesis following challenge. Microorganisms 7:268.
Kanehisa, M., and Y. Sato. 2020. KEGG Mapper for inferring cellular functions from protein sequences. Protein Sci. Publ. Protein Soc. 29:28–35.
Köröskényi, K., E. Duró, A. Pallai, Z. Sarang, D. Kloor, D. Ucker, S. Beceiro, A. Castrillo, A. Chawla, C. A. Ledent, L. Fésüs, and Z. Szondy. 2011. Involvement of adenosine A2A receptors in engulfment-dependent apoptotic cell suppression of inflammation. J. Immunol. Baltim. Md 186:7144–7155 1950.
Liu, H., and R. M. Pope. 2004. Phagocytes: mechanisms of inflammation and tissue destruction. Rheum. Dis. Clin. 30:19–39.
NRC. 1994. Nutrient Requirements of Poultry: Ninth Revised Edition, 1994. The National Academies Press, Washington, DC.
OECD and Food and Agriculture Organization of the United Nations. 2021. OECD-FAO Agricultural Outlook 2021-2030. OECD Publishing, Paris.
Oliveros, J. C. 2007. Venny. An interactive tool for comparing lists with Venn's diagrams. Accessed Oct. 6, 2021. https://bioinfogp.cnb.csic.es/tools/venny/.
OECD/FAO. 2022. *OECD-FAO Agricultural Outlook 2020-2029*. OECD Publishing, Paris, Rome.
Ott, V., M. Fasshauer, A. Dalski, H. H. Klein, and J. Klein. 2002. Direct effects of ciliary neurotrophic factor on brown adipocytes: evidence for a role in peripheral regulation of energy homeostasis. J. Endocrinol. 173:R1–R8.
Perry, F., C. Johnson, B. Aylward, and R. J. Arsenault. 2020. The differential phosphorylation-dependent signaling and glucose immunometabolic responses induced during infection by *Salmonella* Enteritidis and *Salmonella* Heidelberg in chicken macrophage-like cells. Microorganisms 8:1041.
Sathish, K., B. Padma, V. Munugalavadla, V. Bhargavi, K. V. N. Radhika, R. Wasia, M. Sairam, and S. S. Singh. 2004. Phosphorylation of profilin regulates its interaction with actin and poly (l-proline). Cell. Signal. 16:589–596.
Solaymani-Mohammadi, S., and S. M. Singer. 2013. Regulation of intestinal epithelial cell cytoskeletal remodeling by cellular immunity following gut infection. Mucosal Immunol 6:369–378.
Swaggerty, C. L., T. R. Callaway, M. H. Kogut, A. Piva, and E. Grilli. 2019. Modulation of the immune response to improve health and reduce foodborne pathogens in poultry. Microorganisms 7:65–75.
Szklarczyk, D., A. L. Gable, D. Lyon, A. Junge, S. Wyder, J. Huerta-Cepas, M. Simonovic, N. T. Doncheva, J. H. Morris, P. Bork, L. J. Jensen, and C. von Mering. 2019. STRING v11: protein-protein association networks with increased coverage, supporting functional discovery in genome-wide experimental datasets. Nucleic Acids Res 47:D607–D613.
Szondy, Z., Z. Sarang, B. Kiss, É. Garabuczi, and K. Köröskényi. 2017. Anti-inflammatory mechanisms triggered by apoptotic cells during their clearance. Front. Immunol. 8:909.
The UniProt Consortium. 2021. UniProt: the universal protein knowledgebase in 2021. Nucleic Acids Res 49:D480–D489.
Trost, B., J. Kindrachuk, P. Määttänen, S. Napper, and A. Kusalik. 2013. PIIKA 2: an expanded, web-based platform for analysis of kinome microarray data. PLOS One 8:e80837.
Valencia-Expósito, A., I. Grosheva, D. G. Míguez, A. González-Reyes, and M. D. Martín-Bermudo. 2016. Myosin light-chain phosphatase regulates basal actomyosin oscillations during morphogenesis. Nat. Commun. 7:10746.
White, U. A., and J. M. Stephens. 2011. The gp130 receptor cytokine family: regulators of adipocyte development and function. Curr. Pharm. Des. 17:340–346.
Wu, Y.-G., P. Zhou, G.-C. Lan, D. Gao, Q. Li, D.-L. Wei, H.-L. Wang, and J.-H. Tan. 2010. MPF governs the assembly and contraction of actomyosin rings by activating RhoA and MAPK during chemical-induced cytokinesis of goat oocytes. PLOS One 5: e12706.
Würtemberger, J., D. Tchessalova, C. Regina, C. Bauer, M. Schneider, A. J. Wagers, and S. Hettmer. 2020. Growth inhibition associated with disruption of the actin cytoskeleton by Latrunculin A in rhabdomyosarcoma cells. PLOS One 15: e0238572.
Zhang, L., J. Luo, P. Wan, J. Wu, F. Laski, and J. Chen. 2011. Regulation of cofilin phosphorylation and asymmetry in collective cell migration during morphogenesis. Development 138:455–464.
Zhang, S. S., H. G. SU, Z. H. O. U. Ying, X. M. LI, J. H. FENG, and M. H. ZHANG. 2016. Effects of sustained cold and heat stress on energy intake, growth and mitochondrial function of broiler chickens. J. Integr. Agric. 15:2336–2342.